Quantifying the Origin of Released Ag+ Ions from Nanosilver

ARTICLE *in* LANGMUIR · OCTOBER 2012

Impact Factor: 4.46 · DOI: 10.1021/la303370d · Source: PubMed

5 AUTHORS, INCLUDING:

Georgios A. Sotiriou
ETH Zurich
64 PUBLICATIONS **946** CITATIONS
SEE PROFILE

Jesper T. N. Knijnenburg
ETH Zurich
11 PUBLICATIONS **128** CITATIONS
SEE PROFILE

Sotiris E. Pratsinis
ETH Zurich
503 PUBLICATIONS **16,531** CITATIONS
SEE PROFILE

Langmuir

Article

pubs.acs.org/Langmuir

Quantifying the Origin of Released Ag^+ Ions from Nanosilver

Georgios A. Sotiriou,[†] Andreas Meyer,[‡] Jesper T. N. Knijnenburg,[†] Sven Panke,[‡] and Sotiris E. Pratsinis*[,†]

[†]Particle Technology Laboratory, Institute of Process Engineering, Department of Mechanical and Process Engineering, ETH Zurich, Sonneggstrasse 3, CH-8092 Zurich, Switzerland, and [‡]Bioprocess Laboratory, Department of Biosystems Science and Engineering, ETH Zurich, Mattenstrasse 26, CH-4058 Basel, Switzerland

Supporting Information

ABSTRACT: Nanosilver is most attractive for its bactericidal properties in modern textiles, food packaging, and biomedical applications. Concerns, however, about released Ag^+ ions during dispersion of nanosilver in liquids have limited its broad use. Here, nanosilver supported on nanostructured silica is made with closely controlled Ag size both by dry (flame aerosol) and by wet chemistry (impregnation) processes without any surface functionalization that could interfere with its ion release. It is characterized by electron microscopy, atomic absorption spectroscopy, and X-ray diffraction, and its Ag^+ ion release in deionized water is monitored electrochemically. The dispersion method of nanosilver in solutions affects its dissolution rate but not the final Ag^+ ion concentration. By systematically comparing nanosilver size distributions to their equilibrium Ag^+ ion concentrations, it is revealed that the latter correspond precisely to dissolution of one to two surface silver oxide monolayers, depending on particle diameter. When, however, the nanosilver is selectively conditioned by either washing or H_2 reduction, the oxide layers are removed, drastically minimizing Ag^+ ion leaching and its antibacterial activity against *E. coli*. That way the bactericidal activity of nanosilver is confined to contact with its surface rather than to rampant ions. This leads to silver nanoparticles with antibacterial properties that are essential for medical tools and hospital applications.

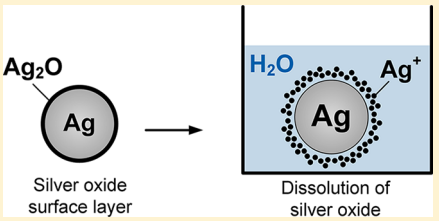

INTRODUCTION

Among engineered nanomaterials in consumer products, nanosilver is the most common[1] for its antibacterial, plasmonic, or electronic properties. At the same time, its bactericidal properties raise concerns for aquatic micro-organisms upon disposal.[2] In fact, not long ago, petitions had been filed to the U.S. EPA to label nanosilver as a pesticide.[3] Even though the number of studies on nanosilver toxicity has grown exponentially since 2006, an understanding of its antibacterial mechanism only now emerges.[4−7] Silver nanoparticles alone can induce toxicity;[8] however, a major role is played by the released Ag^+ ions from their surface upon its contact with water.[6,7,9−11] So the amount of released, leached, or dissolved Ag^+ ions strongly depends on nanosilver particle size[7] because smaller particles release much more Ag^+ ions. In fact, size dictates whether Ag^+ ions or particles are responsible for the nanosilver antibacterial activity.[7] This emphasizes the importance of Ag surface area concentration, rather than mass or number concentrations, in nanosilver dose relations.[5,12]

This Ag^+ ion release is exploited in a variety of target applications and products,[13] so silver nanoparticles, alone or supported on a ceramic support, are used as antimicrobial fillers in textiles[14] and polymers[15] for food-packaging[16] and biomedical applications,[17,18] antimicrobial paints,[19] and potentially for drug delivery.[5] Several factors influence the Ag^+ ion release in aqueous solutions: surface coatings or functionalization, temperature, pH, dissolved oxygen concentration, and the presence of organic matter and other ions[10,11,20−23] including chlorine.[24] Most Ag^+ ion release occurs from oxidation of metallic nanosilver by dissolved oxygen and protons,[25] and actually oxidized silver has stronger antibacterial activity than metallic silver.[5,9,25] However, the performance of nanosilver as antimicrobial agent after its initial employment has not been investigated, prompting further research. Indeed, such an understanding is essential before nanosilver appears not only for specialized treatments in hospitals but also in consumer products for everyday use.[13]

Here, the effect of nanosilver size and surface composition on Ag^+ ion release is investigated systematically by preparing Ag nanoparticles supported on nanostructured SiO_2 by wet impregnation[26] and flame spray pyrolysis (FSP).[7] The nanosilver made here has closely controlled size but does not have any surface functionalization that could compromise the Ag^+ ion release kinetics. The goal is to quantitatively understand the characteristics of nanosilver that influence the Ag^+ ion release and to evaluate how their antibacterial performance is influenced after initial Ag dissolution. This is done by monitoring the Ag^+ ion release from Ag/SiO_2 nanoparticles in aqueous solutions after washing (removal of the leached Ag^+ ion from solution) or reducing them under H_2. The released Ag^+ ion concentration is quantitatively traced to the nanosilver surface layers by a mass balance. Finally, the antibacterial activity of washed and reduced Ag/SiO_2 nanoparticles is explored with *E. coli* bacteria that encode a green fluorescent protein, focusing on nanosilver size and surface treatment.

Received: February 25, 2012
Revised: October 15, 2012
Published: October 16, 2012

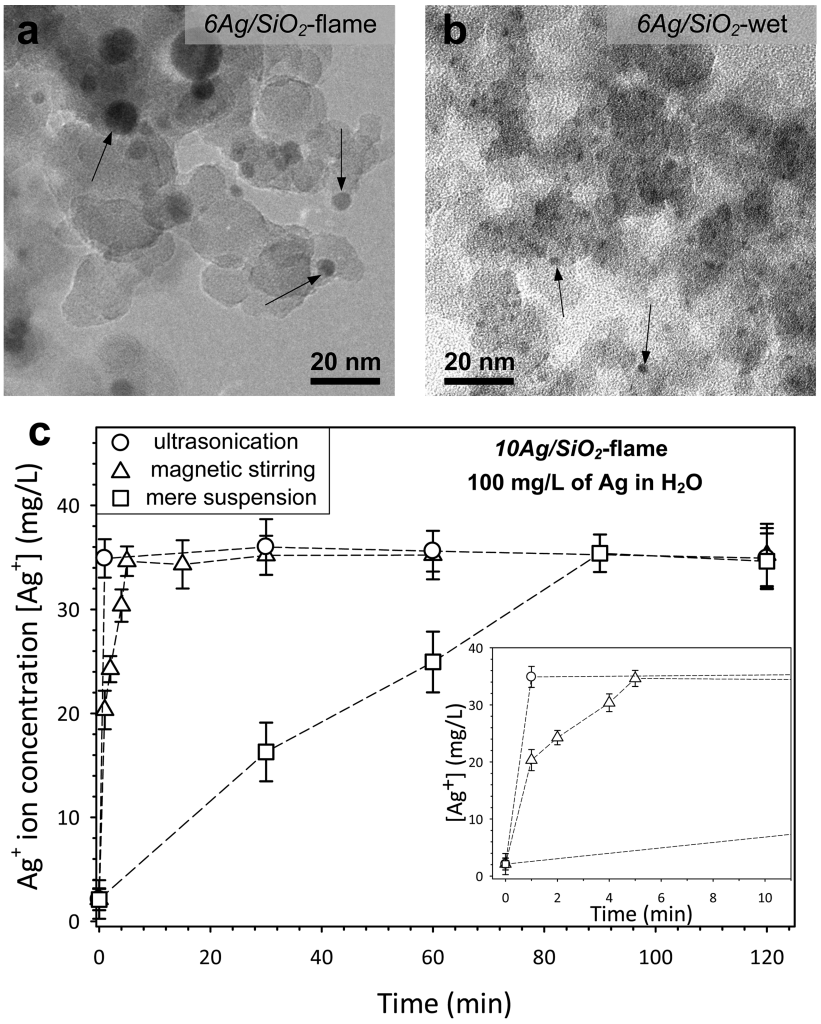

Figure 1. Transmission electron microscopy images of 6Ag/SiO_2 nanoparticles made by dry flame- (a) and wet-chemistry (b) processes. The nanosilver particles are the dark spots shown by the arrows. (c) The evolution of Ag^+ ion concentration in aqueous suspensions of flame-made 10Ag/SiO_2 nanoparticles at Ag mass concentration of 100 mg/L by three different dispersion methods: ultrasonication (○), magnetic stirring at 600 rpm (△), and mere suspension without any agitation (□). The inset magnifies the early stages of dissolution. All suspensions reach identical [Ag^+] regardless of dispersion method, although ultrasonication attains it most rapidly assuring no transport limitations and good nanoparticle dispersion.

MATERIALS AND METHODS

Ag/SiO_2 nanoparticles were made either by FSP[7] or by impregnation[26] of silver nitrate (Aldrich, purity >99%) on nanostructured SiO_2 (Evonik, A300) for various nominal Ag-contents x = 1−50 wt %. Flame-made Ag/SiO_2 nanoparticles were made by flame-spray-pyrolysis (FSP).[7] Silver acetate (Aldrich, purity >99%) and hexamethyldisiloxane (HMDSO, Aldrich, purity >97%) were used as silver and silicon precursors, respectively. Appropriate amounts of silver acetate were dissolved in a 1:1 mixture of 2-ethylhexanoic acid (Aldrich, purity >98%) and acetonitrile (Aldrich, purity >98%). The corresponding amount of HMDSO for a given Ag-content product was added and stirred for a few minutes just before that solution was fed into the FSP reactor. The total precursor (HMDSO and Ag-acetate) concentration was 0.5 M. The precursor solution was fed through the FSP capillary nozzle at 5 mL/min, dispersed to a fine spray by 5 L/min oxygen (Pan Gas, purity >99%), and combusted to produce high-purity Ag/SiO_2 nanoparticles that were collected on a filter downstream.[7]

The wet-made Ag/SiO_2 nanoparticles were made by impregnation[26] of silver nitrate (Aldrich, purity >99%) on nanostructured SiO_2 (Evonik, A300). SiO_2 nanoparticles were dispersed in deionized water, and then the appropriate amount of silver nitrate was added. The mixture was stirred overnight and then dried at 85 °C for 24 h. The dry powder was ground and annealed at 500 °C for 5 h.[26] The mass fraction x of Ag in the flame-made Ag/SiO_2 particles ranged from x = 0−50 wt % (xAg/SiO_2).

All particles were characterized by X-ray diffraction (XRD) on a Bruker AXS D8 Advance diffractometer (Cu K_α, 40 kV, 40 mA). The crystallite sizes were calculated using the Rietveld method and the software TOPAS3. The actual Ag-content x was determined by atomic absorption spectroscopy (AAS). For this, appropriate amounts of xAg/SiO_2 nanoparticles were digested in HNO_3 (1 M) for 24 h at room temperature and then centrifuged (14 000 rpm, 4 min) to remove the undissolved SiO_2. Next, the Ag-content of the supernatant was measured. High-resolution transmission electron microscopy was performed with a CM30ST microscope (FEI; LaB6 cathode, operated at 300 kV, point resolution ∼2 Å). The electron beam could be set to selected areas to determine material composition by energy dispersive X-ray spectroscopy. Particles were dispersed in ethanol and deposited onto a perforated carbon foil supported on a copper grid. Particle size distributions from the TEM analysis were obtained by counting at least 200 particles with the software ImageJ.[12]

The Ag^+ ion concentration of aqueous suspensions was determined by ion selective electrode and an ion meter (both Metrohm).[7] Ag/SiO_2 particles were dispersed in deionized water by ultrasonication (Sonics vibra-cell 600 W, 2 min, 0.5/0.5 s on/off pulse, 75% power), magnetic stirring (600 rpm), and without any stirring. Unless stated otherwise, the Ag^+ ion concentrations correspond to the ones obtained

dx.doi.org/10.1021/la303370d | Langmuir 2012, 28, 15929−15936

by ultrasonication. The washing of xAg/SiO_2 nanoparticles was performed by centrifugation of their aqueous suspensions, removal of supernatant containing the leached Ag^+ ions, and immediate redispersion of nanoparticles in fresh deionized water (without drying them) by ultrasonication (same as above) to avoid air contact and possible reoxidation. With such a process, the as-prepared Ag/SiO_2 nanoparticles are homogeneously dispersed in water, as after their centrifugation they tend to form large flocs on one side of the vial. By sonication, a homogeneous nanoparticle dispersion is made. The dissolved oxygen (DO) concentration was constant at 8.5−8.9 ppm as measured in air-saturated aqueous suspensions by a DO meter (VWR International). All xAg/SiO_2 samples were reduced at 300 °C for 30 min under H_2 (5% H_2 in He) at 5 mL/min. The samples were kept under He atmosphere until they cool and return to ambient conditions for suspension in deionized water.

The oxide surface layer fraction, R, was calculated over the entire nanosilver size distribution (Figure 4 of ref 12) for one or two molecular layers of Ag_2O (density ρ = 7.14 g/cm^3, Ag_2O molecular thickness of 0.46 nm) on the nanosilver surface as:

$$R = \sum n_i \cdot (s_i/m_i)/N \quad (1)$$

where n_i is the number of ith-sized by S/TEM nanosilver particles, s_i is the mass of the surface oxide mono- or bilayer of the ith particle of total mass m_i, and N is the total number of nanosilver particles.

The antibacterial activity of the xAg/SiO_2 nanoparticles was obtained by a growth inhibition assay described in detail elsewhere.[7] In brief, *E. coli* JM101 bacteria synthesizing a green fluorescent protein (GFP) from a plasmid-encoded gene were grown in Luria−Bertani (LB) broth at 37 °C overnight. The culture was subsequently diluted with LB to an optical density (OD) of 0.05 at 600 nm, which corresponds to about 10^7 colony forming units (CFU)/mL. The Ag/SiO_2 nanoparticles were homogeneously dispersed in deionized water by ultrasonication (Sonics vibra-cell 600 W) for 2 min at 75% amplitude with a pulse configuration on/off of 0.5s/0.5s. A batch solution of 40 mg/L was prepared, and with appropriate dilutions the Ag mass concentration varied from 2.5 to 20 mg/L. For the assay, 50 μL of these nanoparticle-containing solutions was added to 50 μL of the diluted bacteria cultures. Bacterial growth was monitored by the fluorescent signal of the GFP (Perkin-Elmer 1420). The data were corrected for background fluorescence and normalized for the control measurement. The error bars for each data point were the standard deviation of at least four measurements.

RESULTS AND DISCUSSION

Ag^+ Ion Release: Dissolution of the Surface Oxide Layer. Figure 1 shows transmission electron microscopy (TEM) images of flame- (a) and wet-made (b) Ag/SiO_2 nanoparticles. The nanosilver corresponds to the dark spots (shown by the arrows) because of its higher atomic number than SiO_2 (diffuse gray) for either flame-[7,27,28] or wet-made[26,27] Ag/SiO_2 nanoparticles and is dispersed homogeneously on the ceramic support (please see Supporting Information, Figure S1). The nanosilver size could be closely controlled from about 4 to 9 nm depending on the Ag-content x in the flame-made xAg/SiO_2 nanoparticles.[7] Higher Ag-content x for the wet-made nanosilver (e.g., x = 10 wt %) resulted in quite large nanosilver particles (d_p > 30 nm), indicating that FSP might offer a finer control of the nanosilver size than wet-methods.[29]

Figure 1c shows the Ag^+ ion concentration, [Ag^+], of aqueous suspensions containing the 10Ag/SiO_2 flame-made nanoparticles at total Ag mass concentration of 100 mg/L as a function of time for three different dispersion methods: by mere suspension without any agitation (□), by gentle magnetic stirring (△), and ultrasonication (○). For all three dispersion methods, the [Ag^+] reached the same value: ∼35 mg/L. Without any agitation, it took 90 min to reach that asymptotic value, while by magnetic stirring it only took 5 min (Figure 1c, inset). By ultrasonication, the [Ag^+] reached its asymptotic value immediately (less than 1 min). Similar results were obtained for the wet-made nanosilver as it reached equilibrium upon 5 min of stirring, indicating that the equilibrium Ag^+ ion concentration is independent of preparation route and particle suspension by stirring or ultrasonication. This almost immediate dissolution within minutes is in contrast to other dissolution studies of nanosilver where it is observed that the [Ag^+] initially increases, reaching a plateau after hours or days, even upon stirring the suspensions.[5,10,11] This is attributed probably to the presence of surface coatings on nanosilver such as polyvinylpyrrolidone[10] or citrate[10,11] that are used to minimize nanosilver agglomeration. Such coatings, however, might influence the Ag^+ ion release kinetics in aqueous suspensions. In fact, such functionalized or coated nanosilver might hinder its surface-dependent antibacterial activity.[4,30] The nanosilver prepared here does not have any coating that could compromise the Ag^+ ion release, as its agglomeration is inhibited by the presence of the SiO_2 support,[7] and the dissolution kinetics are in agreement with similar nanosilver without surface coating.[9] Furthermore, SiO_2 is rather insoluble in water,[31] and the [Ag^+] remains constant over time, indicating also that no Ostwald ripening takes place.[32,33]

The ultrasonication step is essential as it ensures homogeneous nanoparticle dispersion and rapid ion dissolution minimizing any transport limitations. The fact that [Ag^+] reaches immediately its final value after ultrasonication facilitates such investigations and emphasizes that the Ag^+ ion release should be monitored also after nanosilver homogeneous dispersion. It should be noted that perhaps a small fraction of the dissolved nanosilver comes from metal−dioxygen reaction after oxide dissolution[5] and that the aqueous solutions here do not contain any sulfides that would influence the Ag^+ ion release and form insoluble[23,34] Ag_2S on the nanosilver surface that minimizes its antibacterial activity.[35] This indicates that the nanosilver surface is not oxidized further after the dissolution of the initial oxide layer at the present conditions or little, if any, further oxidation occurs. Further oxidation of nanosilver in solution could occur for low pH values or high H_2O_2 concentrations present.[11]

Figure 2a shows the [Ag^+] after 28 days of aqueous suspensions containing 40 mg/L of Ag of as-prepared (open symbols) flame- (circles) and wet-made (triangle) xAg/SiO_2 nanoparticles as a function of the nanosilver average diameter (d_p) determined by electron microscopy.[12] There is clearly a size effect, because for smaller nanosilver more Ag^+ ion leaching takes place.[5,7,25] For example, upon dispersing nanosilver with 4 nm diameter (1Ag/SiO_2) in water, ∼70% of Ag is leached into solution as ions, in agreement with the Ag^+ ion release of similarly sized nanosilver.[7,9,12] This is why Ag^+ ions dominate the antibacterial activity of nanosilver in these sizes (d_p = 4−12 nm) and why surface area concentrations reflect best its dose relations.[7,12] The nanosilver synthesis method does not seem to affect the Ag^+ ion release as the [Ag^+] from wet-made 6Ag/SiO_2 follows the same trend as that from flame-made xAg/SiO_2 for x = 1−50 wt % (Figure 2a).

When the dispersed xAg/SiO_2 nanoparticles are removed by centrifugation[7] from these suspensions and redispersed in fresh deionized water (Figure 2a, washed xAg/SiO_2, filled symbols), the [Ag^+] after 28 days is substantially lower regardless of preparation method. This indicates that the release of Ag^+ ions from washed nanosilver is rather minimal. It is well-known that silver oxide layer formation occurs[26−28] during processing for

dx.doi.org/10.1021/la303370d | *Langmuir* 2012, 28, 15929−15936

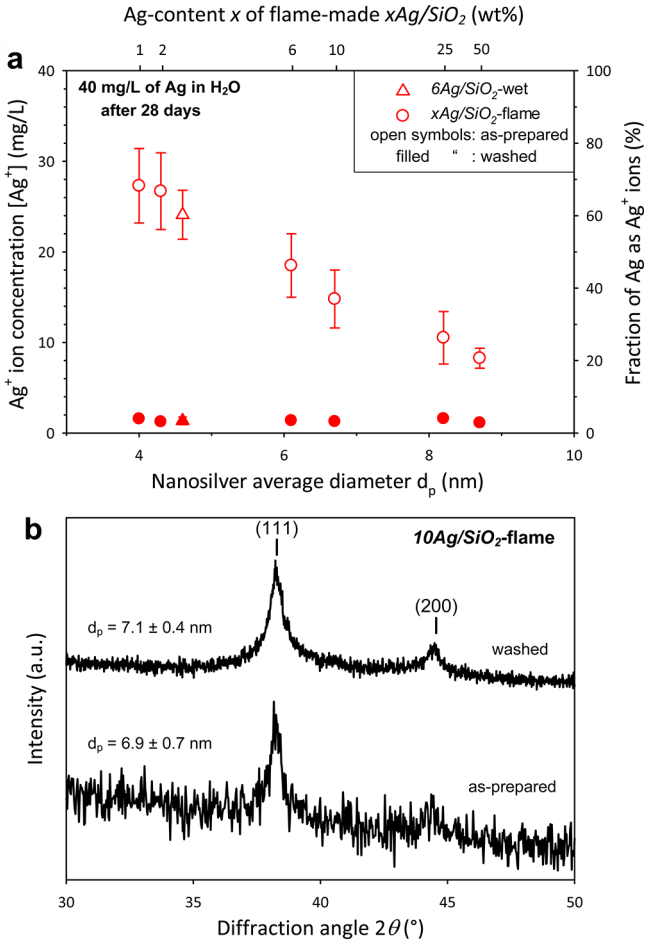

Figure 2. (a) Ag^+ ion concentration $[Ag^+]$ of aqueous suspensions after 28 days that contains the as-prepared (open symbols) and washed (filled symbols) flame- (circles) and wet-made (triangle) xAg/SiO_2 nanoparticles as a function of average nanosilver size (bottom axis) or Ag-content x (top axis) of the flame-made nanoparticles at Ag mass concentration of 40 mg/L. (b) XRD patterns of as-prepared (bottom) and washed (top) flame-made 10Ag/SiO_2 nanoparticles showing that the main diffraction peak of silver metal is similar for both as-prepared and washed nanosilver.

both flame- and wet-made nanosilver that involves high temperatures and exposure to oxygen. Such a silver oxide layer has been detected for Ag/SiO_2 nanoparticles made by FSP[27,28] and wet-impregnation.[26] The initial oxide layer on the surface of nanosilver[26,28] dissolves upon dispersion of the as-prepared Ag/SiO_2 nanoparticles, releasing Ag^+ ions. As soon as, however, this oxide dissolution occurs, the nanosilver particles hardly release more ions (Figure 2a, filled symbols). The presence of an oxide layer on the nanosilver surface is consistent with its oxidative dissolution under aerobic conditions.[11,36]

Figure 2b shows the XRD patterns of the flame-made 10Ag/SiO_2 before (bottom) and after washing (top). The peak positions correspond to Ag metal, while the lack of flat baseline is attributed to the presence of amorphous silica support and silver oxide. There is clearly metallic silver present in the as-prepared flame-made 10Ag/SiO_2 nanoparticles with an average crystal size of 6.9 ± 0.7 nm. After being washed, this sample seems to release almost ~38% of its Ag mass as ions (Figure 2a, open symbols for x = 10 wt % top abscissa). So after washing, its average crystal size should have decreased to 5.9 nm (assuming monodisperse nanosilver). The main diffraction peak around 38°, however, remains similar before and after washing of the nanoparticles. This indicates that the Ag crystal size has not changed after washing, and, in fact, the average crystal size is almost identical within the instrument accuracy (7.1 ± 0.4 nm). The practically identical nanosilver average crystal sizes before and after washing further indicate that the dissolved Ag^+ ions come from the dissolution of amorphous silver oxide layer on the nanosilver surface[5] rather than the dissolution of crystalline nanosilver. This layer cannot be detected by XRD[12] but only by EXAFS[26−28] or XPS[37] as it has been shown for both identical flame-[27,28] and wet-made[26,27] xAg/SiO_2 nanoparticles. The XRD patterns of the washed particles have a slightly better signal-to-noise ratio probably because their amorphous oxide layer has been removed. This increase in the XRD signal-to-noise ratio has been observed also for bare and amorphous silica-coated iron oxide nanoparticles with similar sizes.[38] For x < 6 wt %, reliable XRD patterns could not be obtained as the Ag-content x was too little in the xAg/SiO_2 particles, and thus mostly an amorphous hump was present.[7]

Ag^+ Ion Release: Reduction under H_2 of the Surface Oxide Layer. Figure 3a shows the XRD patterns of before (as-prepared) and after reduction under H_2 of 6Ag/SiO_2 nanoparticles made by wet-chemistry.[26] Before H_2 reduction, there are hardly any peaks corresponding to silver metal or oxides, although a peak seems to emerge at 38°, which, however, can be surely detected after the reduction. This indicates that after reduction, the oxide layer covering the core nanosilver surface becomes metallic, and thus the metallic Ag content increases, enabling its detection by XRD. No Ag enlargement is expected by the high-temperature H_2 reduction (300 °C). Even though temperatures in this range may induce nanosilver growth, the corrugated nanostructured SiO_2 support prevents nanosilver growth by surface diffusion and sintering.[7] Furthermore, the H_2 reduction of these samples indicates the formation of a silver oxide layer on the exposed nanosilver surface, while the formation of silver-silicate at the interface between Ag−SiO_2 cannot be excluded,[27] which, however, does not influence the release of Ag^+ ions.

Figure 3b shows the $[Ag^+]$ for 28 days from solutions containing the as-prepared (open symbols) and reduced under H_2 (filled symbols) 6Ag/SiO_2 nanoparticles made by flame- (circles) and wet- (triangles) processes. The $[Ag^+]$ from reduced 6Ag/SiO_2 nanoparticles is much less than that of as-prepared ones. These $[Ag^+]$ values were also stable for nearly a month (Figure 3b), indicating that the reduced nanosilver particles do not oxidize further when dispersed in deionized water.

Therefore, the release of Ag^+ ions from metallic nanosilver particles is much less than that from nanosilver with oxidized surface.[9] This result also explains why the antibacterial activity of metallic nanosilver is lower than that from oxidized nanosilver,[25] because for such small nanosilver sizes the antibacterial activity is dominated by the released Ag^+ ions.[7] It should also be noted that the $[Ag^+]$ from the reduced xAg/SiO_2 samples is not completely zero (Figure 3b), and actually slightly higher than the washed nanoparticles (Figure 2a), indicating that a small release of Ag^+ ions takes place immediately after their dispersion. This could be attributed to the presence of a small fraction of oxidized Ag layer, as nanosilver may be partially surface oxidized even at ambient conditions.[39]

dx.doi.org/10.1021/la303370d | Langmuir 2012, 28, 15929−15936

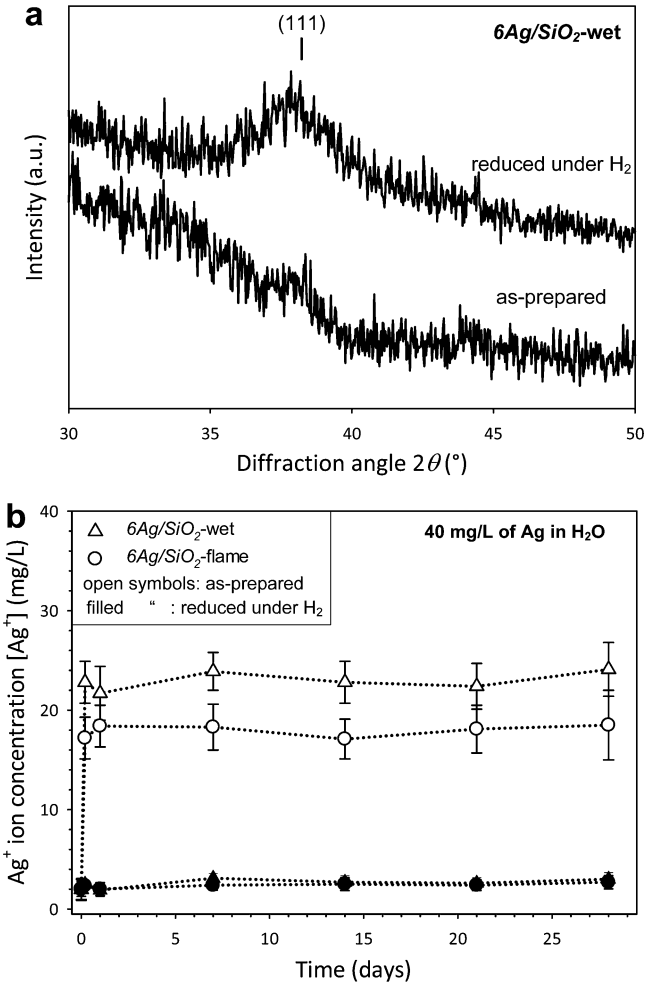

Figure 3. (a) XRD patterns of the as-prepared (bottom) and reduced under H_2 (top) wet-made $6Ag/SiO_2$ nanoparticles. The peak position of the silver metal is also indicated. After reduction, a peak emerges at $2\theta = 38°$ corresponding to silver metal. (b) The $[Ag^+]$ as a function of time for the as-prepared (open symbols) and reduced (filled symbols) wet- (triangles) and flame-made (circles) $6Ag/SiO_2$ nanoparticles. The time = 0 days corresponds to $[Ag^+]$ immediately before the nanoparticle dispersion by ultrasonication, while the second data point corresponds to the $[Ag^+]$ immediately after ultrasonication.

Ag Oxide Layer Thickness and Ag^+ Ion Concentration. Figure 4 shows the Ag mass fraction as Ag^+ ions assuming one (□, dotted line) or two (◇, broken line) silver oxide monolayers on the surface of nanosilver as calculated from the Ag particle size distributions from electron microscopy[12] as a function of nanosilver average diameter, d_p (bottom axis or abscissa), and Ag-content x in the flame-made xAg/SiO_2 particles (top axis or abscissa). Figure 4 also shows the mass fraction of Ag as ions in aqueous suspensions from as-prepared flame- (circles) or wet-made (triangle) xAg/SiO_2 from Figure 2a. For $d_p \geq 8$ nm, the mass fraction of Ag as ions in suspension (solid line) corresponds well to that of a single silver oxide monolayer (dotted line) on the nanosilver surface. For $d_p < 5$ nm, the Ag^+ ion mass fraction (solid line) corresponds asymptotically to the mass from two silver oxide surface layers. An intermediate appears for 5 nm < d_p < 8 nm. Therefore, the leached Ag^+ ions in suspensions can close the mass balance with 1−2 silver oxide layers from the nanosilver surface depending on particle size. This is in agreement with O_2 chemisorption on

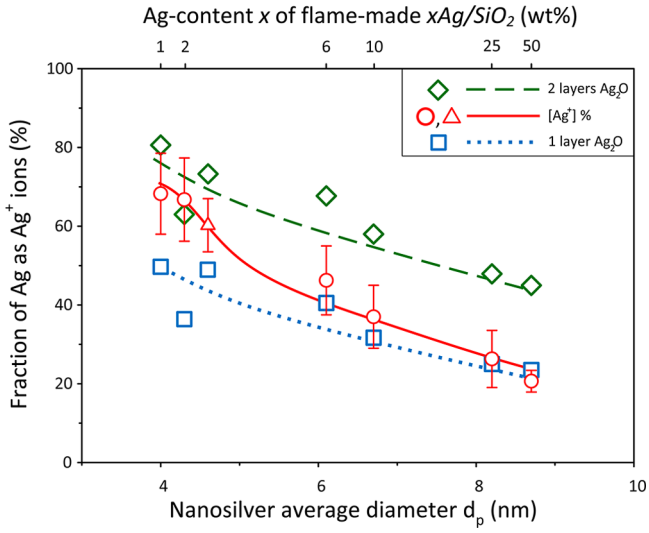

Figure 4. Fraction of Ag atoms as ions in the aqueous suspensions (flame- ○ and wet-made △, solid line) as a function of the nanosilver average diameter (bottom axis), $d_{S/TEM}$, and Ag-content x in the xAg/SiO_2 flame-made nanoparticles (top axis) from Figure 2a. Additionally, the estimated values $[Ag^+]$ as calculated from the nanosilver size distributions assuming 1 layer (□, dotted line) and 2 layers (◇, broken line) of silver oxide on the surface of the nanosilver particles.

such nanosilver, indicating that smaller nanosilver particles oxidize faster than larger ones.[7]

Silver oxide has higher solubility than silver metal in water.[40] As a result, upon dispersion of nanosilver in water, its surface oxide monolayer dissolves quite rapidly as ions (Figure 1c), further indicating that the released Ag^+ ions mostly originate from the leaching (dissolution) of this oxidized layer.[5,7] The existence of 1−2 layers of oxidized Ag on the surface of nanosilver for smaller particles and Ag contents (Figure 4 at d_p < 5 nm) is quite plausible given that smaller nanosilver particles tend to oxidize more than larger ones.[41]

The above result emphasizes the importance of the oxidation state of nanosilver and shows that with flame- or wet-synthesis of nanosilver and subsequent drying and calcination the Ag surface is oxidized. In fact, it is remarkable that with surface treatment (washing or H_2 reduction), the Ag^+ ion release was minimized. This further indicates that by controlling the oxidation state of nanosilver surface, the Ag^+ ion release in aqueous solutions can be controlled.[5,9,25] This origin of the released Ag^+ ions from the silver oxide surface layer also explains the strong size-effect of the Ag^+ ion release of nanosilver; the mass fraction of the silver oxide surface layer becomes progressively larger for a decreasing nanosilver size.

Antibacterial Activity. Figure 5 shows the *E. coli* fluorescence that corresponds to *E. coli* population[7] for 330 min in the presence of as-prepared (open symbols) and washed (filled symbols) flame- (circles) and wet-made (triangles) $6Ag/SiO_2$ nanoparticles (Ag mass concentration C = 2.5 mg/L). The *E. coli* growth in the absence of any nanosilver is also shown (control, ☆).[7] For both as-prepared, flame-, and wet-made nanosilver, *E. coli* growth is completely inhibited. This is attributed to the high amount of Ag^+ ions in solution from both samples (Figure 2a). For the employed nanosilver sizes here, the released Ag^+ ions dominate their antibacterial activity.[7] In the presence, however, of washed $6Ag/SiO_2$ nanoparticles, *E. coli* growth is not significantly affected because the washed nanosilver does not release many Ag^+ ions (Figure 2a), and

dx.doi.org/10.1021/la303370d | Langmuir 2012, 28, 15929−15936

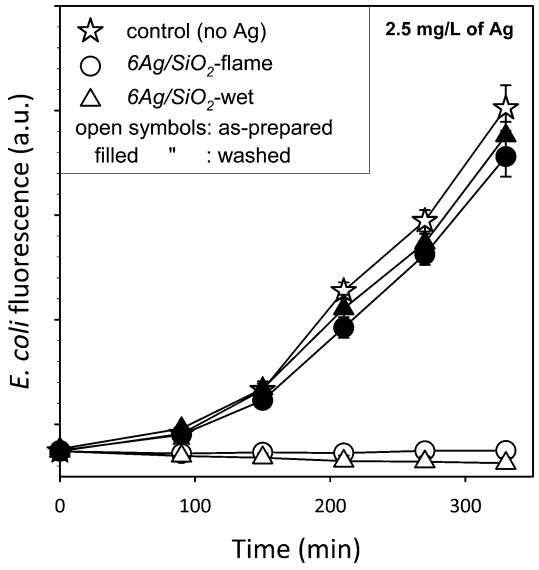

Figure 5. *E. coli* fluorescence (that corresponds to the *E. coli* population) in the presence of as-prepared (open symbols) and washed (filled symbols) flame- (circles) and wet-made (triangles) $6Ag/SiO_2$ nanoparticles for 2.5 mg/L Ag mass concentration. The initial Ag size of the flame- and wet-made from the TEM analysis is 6.1 and 4.6 nm, respectively. The *E. coli* growth in the absence of any nanoparticles is also shown (control, ☆). Error bars correspond to the standard deviation of four measurements for every symbol.

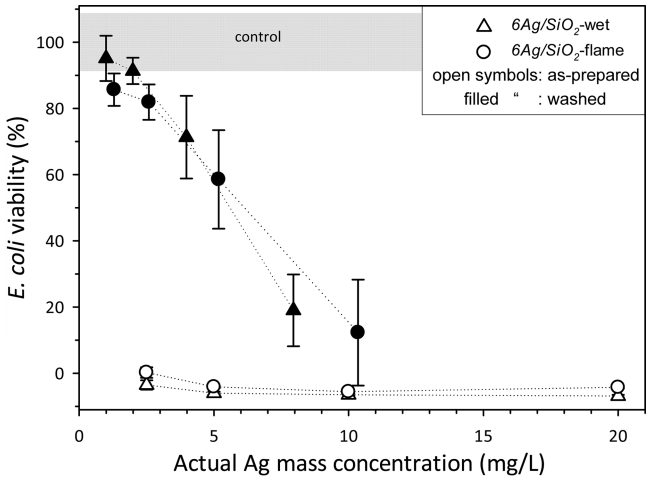

Figure 6. *E. coli* viability (shaded band at 100% corresponds to the control, stars in Figure 5) in the presence of as-prepared (open symbols) and washed (filled symbols) flame- (circles) and wet-made (triangles) $6Ag/SiO_2$ nanoparticles as a function of actual Ag mass concentrations, as calculated from Figure 2a. The error bars correspond to the standard deviation of four measurements.

thus these particles do not induce a strong antibacterial activity for the employed nominal concentration of 2.5 mg/L of Ag.[7,12]

The Ag surface area concentration of this washed nanosilver is almost one-half that of the as-prepared one: 0.062 and 0.130 m^2/L, respectively (please see the Supporting Information for detailed calculations). The *E. coli* growth is not significantly influenced in the presence of the washed nanosilver (Figure 5, filled symbols), even though an *E. coli* growth of about 30% should have been observed for such surface area concentration (0.062 m^2/L) during that period (Figure 8 of ref 12). This further corroborates that the washed nanosilver does not release Ag^+ ions at the same rate as the as-prepared nanosilver of that surface area concentration, in agreement with Figure 2a. Therefore, the antibacterial activity of nanosilver can be controlled and even minimized when its surface is treated. Similar results were obtained in the presence of reduced nanosilver (92−98% *E. coli* viability for Ag mass concentration C = 2.5 mg/L), as they also have a minimal Ag^+ ion release (Figure 3b).

Figure 6 shows the final *E. coli* viability after 330 min (100% corresponds to the control, ☆ from Figure 5) for the as-prepared (open symbols) and washed (filled symbols) flame- (circles) and wet-made (triangles) $6Ag/SiO_2$ nanoparticles as a function of actual Ag mass concentrations. The actual Ag mass concentrations from the washed nanosilver have been calculated taking into account their Ag^+ ion release or leaching as obtained from Figure 2a. For all employed Ag mass concentrations, the $[Ag^+]$ from the as-prepared nanoparticles is high enough to completely inhibit the *E. coli* growth. The slightly negative values obtained for the as-prepared nanosilver most probably originate from photobleaching of media components. On the other hand, the *E. coli* viability of washed nanosilver is much higher than that of as-prepared nanosilver because the former releases much less Ag^+ ions (Figure 2a). As, however, the Ag mass concentration of the washed nanosilver is increased, the latter start exhibiting some antibacterial activity, reducing the cell viability almost completely for Ag mass concentrations larger than 10 mg/L of Ag. The effective $[Ag^+]$ of the washed flame- and wet-made nanosilver ranges from 0.0875 to 0.70 mg/L (Supporting Information). Such low $[Ag^+]$ values can influence bacteria growth, and in fact the antibacterial activity observed here for higher nominal Ag mass concentrations for the washed nanosilver is attributed mainly to the released Ag^+ ions.[12]

So by washing nanosilver, it might be possible to remove the oxide layer from its surface and reuse the washed metallic nanosilver as an antibacterial agent that would exhibit the desired bactericidal properties only by contact with its surface with limited ion leaching. This, of course, would mean that higher Ag concentrations of these washed nanosilver particles need to be used than the as-prepared ones because the antibacterial activity of the latter is stronger than the former for the same Ag mass concentrations. The antibacterial activity of the as-prepared nanosilver, however, may not last longer than the first washing of a textile product, for example, as the oxide layer will be removed. If, however, nanosilver particles that have their surface oxide layers removed are used at sufficiently high Ag concentrations, the antibacterial performance could be maintained even after washing with potentially minimal impact to the environment by Ag^+ ion leaching from metallic nanosilver.

■ CONCLUSIONS

Ag/SiO_2 nanoparticles were made by flame aerosol technology and wet-impregnation. In both cases, the nanosilver particles were homogeneously dispersed on the amorphous SiO_2 support, and their size could be controlled by varying the Ag-content (mass fraction %) x in these xAg/SiO_2 particles. The nanosilver size could be controlled more flexibly by flame technology, and a good agreement between nominal and actual Ag-content x in the xAg/SiO_2 nanoparticles was obtained. The Ag^+ ion release from these xAg/SiO_2 nanoparticles was investigated in deionized water. Dispersing nanosilver in deionized water by mere suspension, magnetic stirring, or

dx.doi.org/10.1021/la303370d | *Langmuir* 2012, 28, 15929−15936

ultrasonication did not affect the final Ag^+ ion concentration, but ultrasonication drastically accelerated attainment of the final Ag^+ ion value, assuring no transport limitations and good suspension of nanosilver.

A higher Ag^+ ion concentration was obtained for smaller nanosilver particles. When, however, these particles were washed and redispersed in water, the Ag^+ ion concentration was minimal. Additionally, the Ag^+ ion release could be controlled by surface treatment (reduction) of the nanosilver, emphasizing the significance of the oxidation state of its surface. The presence of silica here does not influence these results as most nanosilver particles can be readily washed or reduced to remove their oxide layer. It is shown, for the first time to our knowledge, that the release of Ag^+ ions from nanosilver in aqueous solutions corresponds to the mass leached or dissolved of one or two oxidized monolayers from its surface depending on nanosilver size. The antibacterial activity against *E. coli* of small (<10 nm) nanosilver particles that have their silver oxide surface layer either removed by dissolution or reduced to metallic silver is significantly lower than that of as-prepared nanosilver particles. This understanding may help engineer nanosilver products that retain their antibacterial activity mostly by the nanosilver contact, while the release of toxic Ag^+ ions can be controlled facilitating the broader use of nanosilver, for example, as fillers in textiles or polymers for biomedical uses (e.g., catheters).

■ ASSOCIATED CONTENT

Supporting Information

Determination of the actual Ag-content in the samples by acidic dissolution and atomic absorption spectroscopy. Calculations regarding the effective Ag^+ ion, Ag mass, and Ag surface area concentrations. This material is available free of charge via the Internet at http://pubs.acs.org.

■ AUTHOR INFORMATION

Corresponding Author

*E-mail: pratsinis@ptl.mavt.ethz.ch.

Notes

The authors declare no competing financial interest.

■ ACKNOWLEDGMENTS

We thank Dr. Frank Krumeich for the electron microscopy (ETH Zurich). Financial support from the Swiss National Science Foundation (no. 200020-126694) and the European Research Council is kindly acknowledged.

■ REFERENCES

(1) Project on Emerging Nanotechnologies. www.nanotechproject.org; accessed June 2012.

(2) Lee, B. G.; Griscom, S. B.; Lee, J. S.; Choi, H. J.; Koh, C. H.; Luoma, S. N.; Fisher, N. S. Influences of Dietary Uptake and Reactive Sulfides on Metal Bioavailability from Aquatic Sediments. *Science* **2000**, *287*, 282−284.

(3) Erickson, B. E. Nanosilver Pesticides. *Chem. Eng. News* **2009**, *87*, 25−26.

(4) Auffan, M.; Rose, J.; Bottero, J.-Y.; Lowry, G. V.; Jolivet, J.-P.; Wiesner, M. R. Towards a Definition of Inorganic Nanoparticles from an Environmental, Health and Safety Perspective. *Nat. Nanotechnol.* **2009**, *4*, 634−641.

(5) Liu, J. Y.; Sonshine, D. A.; Shervani, S.; Hurt, R. H. Controlled Release of Biologically Active Silver from Nanosilver Surfaces. *ACS Nano* **2010**, *4*, 6903−6913.

(6) Navarro, E.; Piccapietra, F.; Wagner, B.; Marconi, F.; Kaegi, R.; Odzak, N.; Sigg, L.; Behra, R. Toxicity of Silver Nanoparticles to *Chlamydomonas Reinhardtii*. *Environ. Sci. Technol.* **2008**, *42*, 8959−8964.

(7) Sotiriou, G. A.; Pratsinis, S. E. Antibacterial Activity of Nanosilver Ions and Particles. *Environ. Sci. Technol.* **2010**, *44*, 5649−5654.

(8) Morones, J. R.; Elechiguerra, J. L.; Camacho, A.; Holt, K.; Kouri, J. B.; Ramirez, J. T.; Yacaman, M. J. The Bactericidal Effect of Silver Nanoparticles. *Nanotechnology* **2005**, *16*, 2346−2353.

(9) Gunawan, C.; Teoh, W. Y.; Marquis, C. P.; Lifia, J.; Amal, R. Reversible Antimicrobial Photoswitching in Nanosilver. *Small* **2009**, *5*, 341−344.

(10) Kittler, S.; Greulich, C.; Diendorf, J.; Koller, M.; Epple, M. Toxicity of Silver Nanoparticles Increases During Storage Because of Slow Dissolution under Release of Silver Ions. *Chem. Mater.* **2010**, *22*, 4548−4554.

(11) Liu, J. Y.; Hurt, R. H. Ion Release Kinetics and Particle Persistence in Aqueous Nano-Silver Colloids. *Environ. Sci. Technol.* **2010**, *44*, 2169−2175.

(12) Sotiriou, G. A.; Teleki, A.; Camenzind, A.; Krumeich, F.; Meyer, A.; Panke, S.; Pratsinis, S. E. Nanosilver on Nanostructured Silica: Antibacterial Activity and Ag Surface Area. *Chem. Eng. J.* **2011**, *170*, 547−554.

(13) Sotiriou, G. A.; Pratsinis, S. E. Engineering Nanosilver as an Antibacterial, Biosensor and Bioimaging Material. *Curr. Opin. Chem. Eng.* **2011**, *1*, 3−10.

(14) Height, M. J.; Pratsinis, S. E. Antimicrobial and Antifungal Powders Made by Flame Spray Pyrolysis. European Patent EP1846327 (A1), 2007.

(15) Kong, H.; Jang, J. Antibacterial Properties of Novel Poly(Methyl Methacrylate) Nanofiber Containing Silver Nanoparticles. *Langmuir* **2008**, *24*, 2051−2056.

(16) Loher, S.; Schneider, O. D.; Maienfisch, T.; Bokorny, S.; Stark, W. J. Micro-Organism-Triggered Release of Silver Nanoparticles from Biodegradable Oxide Carriers Allows Preparation of Self-Sterilizing Polymer Surfaces. *Small* **2008**, *4*, 824−832.

(17) Kumar, R.; Munstedt, H. Silver Ion Release from Antimicrobial Polyamide/Silver Composites. *Biomaterials* **2005**, *26*, 2081−2088.

(18) Schiffman, J. D.; Wang, Y.; Giannelis, E. P.; Elimelech, M. Biocidal Activity of Plasma Modified Electrospun Polysulfone Mats Functionalized with Polyethyleneimine-Capped Silver Nanoparticles. *Langmuir* **2011**, *27*, 13159−13164.

(19) Kumar, A.; Vemula, P. K.; Ajayan, P. M.; John, G. Silver-Nanoparticle-Embedded Antimicrobial Paints Based on Vegetable Oil. *Nat. Mater.* **2008**, *7*, 236−241.

(20) Sotiriou, G. A.; Hirt, A. M.; Lozach, P. Y.; Teleki, A.; Krumeich, F.; Pratsinis, S. E. Hybrid, Silica-Coated, Janus-Like Plasmonic-Magnetic Nanoparticles. *Chem. Mater.* **2011**, *23*, 1985−1992.

(21) Sotiriou, G. A.; Sannomiya, T.; Teleki, A.; Krumeich, F.; Vörös, J.; Pratsinis, S. E. Non-Toxic Dry-Coated Nanosilver for Plasmonic Biosensors. *Adv. Funct. Mater.* **2010**, *20*, 4250−4257.

(22) Fabrega, J.; Fawcett, S. R.; Renshaw, J. C.; Lead, J. R. Silver Nanoparticle Impact on Bacterial Growth: Effect of pH, Concentration, and Organic Matter. *Environ. Sci. Technol.* **2009**, *43*, 7285−7290.

(23) Levard, C.; Reinsch, B. C.; Michel, F. M.; Oumahi, C.; Lowry, G. V.; Brown, G. E. Sulfidation Processes of PVP-Coated Silver Nanoparticles in Aqueous Solution: Impact on Dissolution Rate. *Environ. Sci. Technol.* **2011**, *45*, 5260−5266.

(24) Choi, O.; Cleuenger, T. E.; Deng, B. L.; Surampalli, R. Y.; Ross, L.; Hu, Z. Q. Role of Sulfide and Ligand Strength in Controlling Nanosilver Toxicity. *Water Res.* **2009**, *43*, 1879−1886.

(25) Lok, C. N.; Ho, C. M.; Chen, R.; He, Q. Y.; Yu, W. Y.; Sun, H.; Tam, P. K. H.; Chiu, J. F.; Che, C. M. Silver Nanoparticles: Partial Oxidation and Antibacterial Activities. *J. Biol. Inorg. Chem.* **2007**, *12*, 527−534.

(26) Shimizu, K.; Miyamoto, Y.; Satsuma, A. Silica-Supported Silver Nanoparticles with Surface Oxygen Species as a Reusable Catalyst for Alkylation of Arenes. *ChemCatChem* **2010**, *2*, 84−91.

(27) Beier, M. J.; Schimmoeller, B.; Hansen, T. W.; Andersen, J. E. T.; Pratsinis, S. E.; Grunwaldt, J. D. Selective Side-Chain Oxidation of Alkyl Aromatic Compounds Catalyzed by Cerium Modified Silver Catalysts. *J. Mol. Catal. A: Chem.* **2010**, *331*, 40−49.
(28) Hannemann, S.; Grunwaldt, J. D.; Krumeich, F.; Kappen, P.; Baiker, A. Electron Microscopy and EXAFS Studies on Oxide-Supported Gold-Silver Nanoparticles Prepared by Flame Spray Pyrolysis. *Appl. Surf. Sci.* **2006**, *252*, 7862−7873.
(29) Height, M. J.; Pratsinis, S. E.; Mekasuwandumrong, O.; Praserthdam, P. Ag-ZnO Catalysts for UV-Photodegradation of Methylene Blue. *Appl. Catal., B* **2006**, *63*, 305−312.
(30) Carlson, C.; Hussain, S. M.; Schrand, A. M.; Braydich-Stolle, L. K.; Hess, K. L.; Jones, R. L.; Schlager, J. J. Unique Cellular Interaction of Silver Nanoparticles: Size-Dependent Generation of Reactive Oxygen Species. *J. Phys. Chem. B* **2008**, *112*, 13608−13619.
(31) Alexander, G. B.; Heston, W. M.; Iler, R. K. The Solubility of Amorphous Silica in Water. *J. Phys. Chem.* **1954**, *58*, 453−455.
(32) Harada, M.; Katagiri, E. Mechanism of Silver Particle Formation During Photoreduction Using in situ Time-Resolved SAXS Analysis. *Langmuir* **2010**, *26*, 17896−17905.
(33) Chen, M.; Feng, Y.-G.; Wang, X.; Li, T.-C.; Zhang, J.-Y.; Qian, D.-J. Silver Nanoparticles Capped by Oleylamine: Formation, Growth, and Self-Organization. *Langmuir* **2007**, *23*, 5296−5304.
(34) Liu, J.; Pennell, K. G.; Hurt, R. H. Kinetics and Mechanisms of Nanosilver Oxysulfidation. *Environ. Sci. Technol.* **2011**, *45*, 7345−7353.
(35) Reinsch, B. C.; Levard, C.; Li, Z.; Ma, R.; Wise, A.; Gregory, K. B.; Brown, G. E.; Lowry, G. V. Sulfidation of Silver Nanoparticles Decreases Escherichia Coli Growth Inhibition. *Environ. Sci. Technol.* **2012**, *46*, 6992−7000.
(36) Xiu, Z.-m.; Zhang, Q.-b.; Puppala, H. L.; Colvin, V. L.; Alvarez, P. J. J. Negligible Particle-Specific Antibacterial Activity of Silver Nanoparticles. *Nano Lett.* **2012**, *12*, 4271−4275.
(37) Fragala, M. E.; Compagnini, G.; Malandrino, G.; Spinella, C.; Puglisi, O. Silver Nanoparticles Dispersed in Polyimide Thin Film Matrix. *Eur. Phys. J. D* **1999**, *9*, 631−633.
(38) Teleki, A.; Suter, M.; Kidambi, P. R.; Ergeneman, O.; Krumeich, F.; Nelson, B. J.; Pratsinis, S. E. Hermetically Coated Superparamagnetic Fe_2O_3 Particles with SiO_2 Nanofilms. *Chem. Mater.* **2009**, *21*, 2094−2100.
(39) Schmidt, M.; Masson, A.; Bréchignac, C. Oxygen and Silver Clusters: Transition from Chemisorption to Oxidation. *Phys. Rev. Lett.* **2003**, *91*, 243401.
(40) Lide, D. R. *CRC Handbook of Chemistry and Physics*, 89th (Internet version) ed.; CRC Press/Taylor and Francis: Boca Raton, FL, 2010.
(41) Ivanova, O. S.; Zamborini, F. P. Size-Dependent Electrochemical Oxidation of Silver Nanoparticles. *J. Am. Chem. Soc.* **2010**, *132*, 70−72.